Supplemental Material and Methods

Liver specific *Flvcr1a* knock-out mice generation

The targeting construct to generate a *Flvcr1a* floxed allele, was designed as follows: the first exon of *Flvcr1a* gene was flanked with loxP sites and the neomycin resistance gene, flanked with Flippase Recognition Target (FRT) sites to permit its excision, was inserted in the first intron. This construct was introduced by electroporation into mouse ES cells. Homologous recombination was confirmed by southern blot and ES cells carrying $Flvcr1a^{fl\text{-}neo}$ allele were injected into C57 blastocysts to generate germ-line chimeras. The neomycin resistance cassette in the targeting construct was removed by crossing heterozygous $Flvcr1a^{+/fl\text{-}neo}$ mice with mice carrying the FLP recombinase under the control of the actin promoter (kindly provided by Rolf Sprengel) to produce mice carrying the *Flvcr1a* floxed allele. $Flvcr1a^{fl/fl}$ mice were crossed to mice expressing the Cre recombinase under the control of the Albumin promoter (*alb-cre*) to generate $Flvcr1a^{fl/fl}$*;alb-cre* mice.

Mice and Treatments

Mice used in these studies were 2/3 or 6-month-old littermates on a mixed C57BL/6Jx129Sv background. Knock-in HbS Sickle Cell Anemia mice and $Hbb^{th1/th1}$ β-Thalassemia mice were previously described (1). Both males and females were used in these studies. They were maintained on a standard chow diet and kept with free access to food and water. All experiments were approved by the animal ethical committee of the University of Torino (Italy).

To assess the role of FLVCR1a in the liver mice were treated with Phenylhydrazine (PHZ), Hemin or ALA. In addition they were treated with Dexamethasone, Be(a)P and Imidazole alone

or together with the inhibitor of heme synthesis Succynilacetone (2) and DL-Penicillamine (3). Mice used for different treatments were 2/3 month-old littermates.

Mice were administered 25 mg/kg PHZ (dissolved in PBS, pH at 7.4) intraperitoneally (i.p.), twice a week for one month. Mice received 30μmol/kg freshly prepared hemin intravenously and sacrificed 6 hrs later. Hemin (Frontier Scientific, Logan, Utah) was dissolved in 0.1N NaOH and pH was adjusted at 7.4. Animals were injected i.p. with 120mg/kg ALA (dissolved in PBS) and sacrificed 8 hrs later. Mice were injected i.p. with 75 mg/kg Dexamethasone or 20mg/kg Be(a)P and sacrificed 8/16/32 hrs later. Dexamethasone and Be(a)P were dissolved in corn oil. Animals received 400 mg/kg, i.p., Imidazole (in PBS) over 4 days and sacrificed 24 hrs after the last injection. Some animals were treated with Dexamethasone/Be(a)P/Imidazole plus Succynilacetone 120 mg/kg or DL-Penicillamine 100 mg/kg. Control animals were injected with PBS or corn oil accordingly to the vehicle used to dissolve the agent used for the treatment. Animals were anesthetized and transcardially perfused with PBS to remove blood. Tissue samples were collected and kept frozen until analysis.

Primary Hepatocyte culture preparation and treatment

Hepatocytes were isolated from single hepatic lobules (4). After liver dissection, the single liver lobe was perfused using Hepatocyte Liver Perfusion Medium and then Hepatocyte Liver Digest Medium (Life Technologies Italia, Monza MB, Italy). Perfusion with Digest Medium was kept until the liver lobe felt very soft. This is a critical step, as this medium contains collagenase, and excessive digestion should be avoided to prevent cell death. Subsequently, the perfused liver lobe was disrupted and the cell suspension was forced through a 100 μm Cell Strainer (BD, Becton Dickinson Italia, Milano, Italy). Cells were centrifuged and then cell suspension was applied over a Percoll gradient. After Percoll gradient centrifugation the two upper layers that contain cell

debris and non-parenchymal cells were carefully pipetted out and discarded. Then, the lowest layer that contains the live hepatocytes was collected. Cells were washed, centrifuged and then plated onto collagen-coated well plates. Primary hepatocytes were treated with 5mM ALA or 5mM ALA plus 0.5mM Succynilacetone for 30 minutes for heme uptake experiments or for 8 hrs for ROS production assay.

FLVCR1a-overexpressing HepG2 Cell Line

HepG2 cells were transduced with a lentiviral vector carrying the human Flvcr1a cDNA fused to the Myc epitope to obtain a cell line overexpressing the Flvcr1a-Myc protein. Control HepG2 cells were transduced with a control lentiviral vector. For localization experiments, we performed immunofluorescence on overexpressing and control HepG2 cells using the cell membrane marker WGA (Life Technologies), an antibody against Myc (produced in our laboratory) and one against ZO-1 (Life Technologies).

Heme Content

Heme content in tissues and in bile samples was quantified fluorometrically by the method of Sassa (5). Briefly, tissues were homogenized in phosphate buffer saline (PBS) and protein content was determined by using the Bio-Rad protein assay system (Bio-Rad, Munchen, Germany). Ten μg of protein samples were incubated with 0.5 ml of 2 M Oxalic Acid (Sigma-Aldrich, Milano, Italy) at 95°C for 30 min. Samples were subsequently centrifuged at 14000 rpm for 5 min. Fluorescence emission in the supernatant was determined spectrofluorimetrically (Glomax, Promega Italia). Excitation and emission wavelengths were set at 405 and 662 nm, respectively. The background was evaluated by measuring fluorescence in non-boiled samples. A

standard curve of hemin was run in parallel. Using this method, heme content was measured in primary hepatocytes, total liver extract and hepatic cytosolic and microsomal fractions.

Tissue Iron Measurement

Tissue non-heme iron content determined with a colorimetric method using 4,7-diphenyl-1, 10-phenantroline disulphonic acid (BPS) as chromogen (6). Briefly, 0.1 g of dry tissue was incubated overnight in a mixture of trichloroacetic (10%) and hydrochloric (4N) acids, and 100 µl of supernatant reduced with thioglycolic acid (Sigma-Aldrich) and acetic acid-acetate buffer (pH4.5). Ferrous iron content was determined spectrophotometrically at 535 nm following addition of BPS and incubation for 1 hr at 37ºC. Results were expressed as µg iron/g dry tissue weight.

HO Activity Assay

HO activity was measured by spectrophotometric determination of bilirubin produced from hemin added as the substrate (1). Liver samples were lysed with a hypotonic buffer (0.1 M potassium phosphate, 2mM $MgCl_2$, Complete Protease Inhibitor Cocktail, Roche Diagnostics Corp., Milano, Italy, pH 7.4) for 15' on ice. After brief sonication. 0.6 M sucrose was added to cell lysates in order to obtain an hysotonic solution (final 0.25 M sucrose). Lysates were centrifuged at 1000 x g for 10 min at 4°C to pellet nuclei, and supernatants centrifuged at 12000 x g for 15 min at 4 °C to pellet mitochondria. Finally, supernatants were ultracentrifuged at 105000 x g for 1 hour at 4°C. Microsomal fractions were resuspended in 100 mM potassium phosphate buffer pH 7.4, containing 2 mM $MgCl_2$ and Complete protease inhibitor. Protein concentration was determined using a small aliquot of these suspensions (Bio-Rad, Munchen, Germany). The microsomal supernatant fraction (cytosol) from the liver of a normal rat served as

source of biliverdin reductase. Liver supernatant was prepared fresh from rat liver by homogenization in 0.1 M sodium citrate buffer, pH 5, containing 10% glycerol. HO-1 activity assay was carried out by incubating 600 μg microsome proteins with a reaction mixture containing 1 mM NADPH, 2 mM glucose-6-phosphate, 1U glucose-6-phosphate dehydrogenase (Sigma-Aldrich), 25 μM hemin, 2 mg of rat-liver cytosol and 100 mM potassium phosphate buffer, pH 7.4 (400 μl final volume). The reaction was conducted in the dark for 1h at 37 °C and terminated by placing tubes on ice for 2 min. The amount of bilirubin was determined by the difference in absorption between 464 and 530 nm (extinction coefficient, 40 mM^{-1} cm^{-1} for bilirubin). HO activity was expressed in picomoles of bilirubin formed per milligram microsomal protein per hour.

Bilirubin concentration in bile

Direct and Total bilirubin concentrations in bile were determined colorimetrically using the QuantiChrom bilirubin assay kit DIBR-180 from BioAssay Systems (Hayward, CA). For bile collection, an upper midline laparotomy was realized, the cystic duct was ligated and transected and a cholecystectomy performed. Gallbladder was removed and its volume was determined by water displacement. Bile was collected and stored at -20°C until analysis (1).

Lipid Peroxidation Assay

Lipid peroxidation from tissue extracts was measured using the colorimetric assay kit Bioxytech LPO-586 from Oxis International (Portland, OR), according to the manufacturer's instructions.

Measurement of intracellular ROS accumulation

Accumulation of ROS in primary hepatocytes was assessed by using the oxidant-sensitive fluorescent dye 29,79-dichlorodihydrofluoroscein diacetate (H_2DCFDA; Molecular Probes, Inc., Eugene, OR) (1). H_2DCFDA penetrates easily into the cells. Upon crossing the cellular membrane, H_2DCFDA undergoes deacetylation by intracellular esterases producing a non-fluorescent compound that becomes highly green fluorescent following oxidation by intracellular reactive oxygen species. Within the cell, the probe reacts with ROS to form fluorescent 28,78 dichlorofluoroscein (DCF), which is detected by fluorometry. Primary hepatocytes untreated or treated with ALA or ALA plus SA were incubated with 5μM H_2DCFDA in Hanks' balanced salt solution (HBSS) for 30 min at 37 ℃ under 5% CO_2 atmosphere. Fluorescence was recorded at excitation and emission wavelengths of 485 and 530 respectively by a fluorimeter plate reader (Promega). The background fluorescence caused by buffer and DCF was subtracted from the total fluorescence in each well generated by cells in presence of DCF. Fluorescence intensity units were normalized by mg protein and expressed as arbitrary fluorescence units/mg protein.

ALAS Activity Assay

d -ALAS activity in the liver was assayed according to the methods of Marver *et al*. (7) with minor modification. Briefly, the livers were washed in cold saline, minced, and homogenized in 3 volumes of cold 10 m*M* Tri-HCl buffer, pH 7.4, containing 0.9% NaCl and 0.05 m*M* EDTA. A 16-ml reaction mixture consisting of 4 ml of 240 m*M* Tris-HCl, pH 8.0, 2 ml of 80 m*M* EDTA, 2 ml of 800 m*M* glycine, and 8 ml of liver homogenate was incubated for 1 h at 37°C. Reactions were terminated by adding 4 ml of 12.5% trichloroacetic acid solution, and the samples were centrifuge d at 140 3 *g* for 10 min. The supernatant was further centrifug ed at 10,000 3 *g* for 10 min. To 16 ml of the resultant supernata nt, 0.8 ml 2.5 *N* NaOH, 16 ml 1 *M* sodium acetate

buffer, pH 4.6, and 0.8 ml of acetylace tone were added, and then the mixture solution was heated in boiling water for 20 min. After cooling at ambient temperatures, the sample solution was applied to a Dowex 1-X8 resin (Muromachi Chemicals, Kyoto, Japan) column (3 ml). The column was washed with 15 ml of water, 12 ml of 50% methanol in water, and 12 ml of 1 *M* acetic acid solution, and then eluted with glacial acetic acid. A first run (1 ml) of the elution was discarded , and the subsequen t eluent (3 ml) was collected . To each fraction, the same volume of Ehrlich' s reagent was added, and the mixture solution was allowed to stand for 20 min at room temperature. The resultant reactant of *d* –aminolevulinic acid was spectrophotometrically measured at 553 nm.

CYP1A1 Activity Assay

CYP1A1 activity was assessed by measuring Ethoxyresorufin-O-deethylase (EROD) activity in liver microsomes using 7-ethoxyresorufin as a substrate (8). Liver microsomes (120 μg protein) were added to a reaction mixture of 0.1 M potassium phosphate buffer (pH 7.4) and 1.5 μM 7-ethoxyresorufin. The reaction was started by the addition of 0.5 mM nicotinamide adenine dinucleotide phosphate (NADPH) in a final volume of 1 mL. After incubation at 25°C for 5 min, increase in fluorescence was recorded with excitation and emission wavelengths fixed at 535 nm and 585 nm, respectively.

CYP2E1 Activity Assay

CYP2E1 activity was determined by assaying the hydroxylation of p-nitrophenol to 4-nitrocatechol in the liver microsomal fraction (9). The CYP2E1 assay was performed by incubating 200 μg of microsomal protein for 30 min at 37°C in a volume of 0.5 ml containing 0.1 mM p-nitrophenol, and 1 mM NADPH. The reaction was finished by addition of 0.1 ml of 20%

trichloroacetic acid and the mixture was centrifuged to remove precipitated proteins. 0.5 ml of the supernatant was added to 0.25 ml of 2 M NaOH in a spectrophotometer cuvette and the absorbance read at 535 nm.

Supplemental Results, Figures and Tables

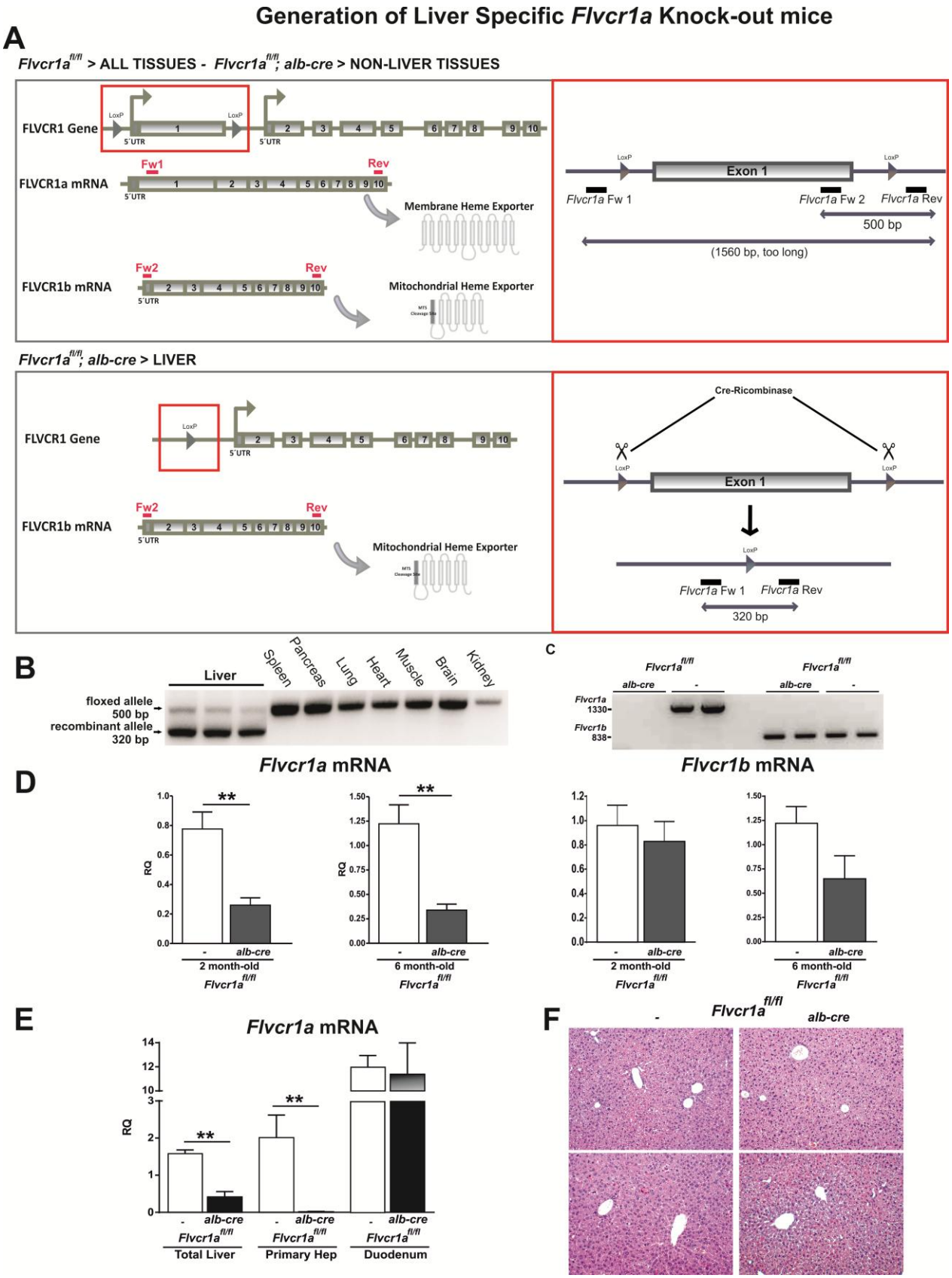

Figure S1. Generation of liver specific *Flvcr1a* knockout mice. (A) Representative scheme of the strategy used to generate liver-specific *Flvcr1a*-null mice. The *Flvcr1a*$^{fl/fl}$ mouse, carrying two loxP sites flanking the exon 1 of *Flvcr1a,* was crossed with the *alb-cre* mouse to obtain a mouse with the specific deletion of the exon 1 of *Flvcr1a* in the liver. The primers, Forward 1, Forward 2 and Reverse, used to verify the deletion of the exon 1 on genomic DNA are depicted on the right. The floxed allele is expected to give rise to a 500 bp band, the recombinant allele to a 320 bp band. The expected *Flvcr1* transcripts and proteins are reported on the left; the primers, Forward 1, Forward 2 and Reverse, used to verify *Flvcr1a* and *Flvcr1b* mRNA expression are indicated in red. (B) Representative PCR on genomic DNA from different tissues of *Flvcr1a*$^{fl/fl}$*;alb-cr*e mice with primers reported in panel A. Obtained bands correspond to those predicted. (C) Representative RT-PCR on cDNA from the liver of *Flvcr1a*$^{fl/fl}$ and *Flvcr1a*$^{fl/fl}$*;alb-cr*e mice with primers indicated in red in (A). In the liver of *Flvcr1a*$^{fl/fl}$*;alb-cr*e mice the excision of the first exon gives rise only to the *Flvcr1b* transcript and not to other truncated mRNAs. (D) qRT-PCR analysis of *Flvcr1a* and *Flvcr1b* mRNA level in the liver of 2 and 6 month-old *Flvcr1a*$^{fl/fl}$ and *Flvcr1a*$^{fl/fl}$*;alb-cr*e mice, n=6. (E) qRT-PCR analysis of *Flvcr1a* mRNA level in total liver, primary hepatocytes and duodenum from 2 month-old *Flvcr1a*$^{fl/fl}$ and *Flvcr1a*$^{fl/fl}$*;alb-cr*e mice, n=4 (bottom). Unpaired T-test analysis with Welch's correction was performed on data reported in Figure S1D,E. RQ: Relative Quantity. (F) Representative liver sections of 6 month-old *Flvcr1a*$^{fl/fl}$ and *Flvcr1a*$^{fl/fl}$*;alb-cr*e mice, stained with Ematossilin and Eosin. No obvious abnormalities was observed in *Flvcr1a*$^{fl/fl}$*;alb-cre* mice. Scale bar: 300μm. **P<0.01.

Blood Analysis	*Flvcr1a* $^{flox/flox}$	*Flvcr1a* $^{flox/flox}$*;alb-cre*
WBC (*10^3 cells/μl)	4,69 ± 1,95	5,55 ± 0,63
RBC (*10^6 cells/μl)	8,68 ± 0,5	9,10 ± 1,07
HGB (g/dL)	12,38 ± 1,02	13,05 ± 1,11
HCT %	41,14 ± 2,75	42,45 ± 5,45
MCV (f/L)	47,07 ± 1,09	46,72 ± 1,45
PLT (*10^3 cells/ml)	1136 ± 648,59	1074 ± 680,67
ALT (U/L)	42,25 ± 15,32	36,6 ± 14,46
AST (U/L)	89 ± 8,48	85 ± 7,7

Table S1. *Flvcr1a*$^{fl/fl}$*;alb-cre* mice do not show difference in blood parameters. Analysis of blood samples from 6 month-old *Flvcr1a*$^{fl/fl}$ and *Flvcr1a*$^{fl/fl}$*;alb-cre* mice (n=6). Values represent mean ± SEM. WBC: white blood cells; RBC: red blood cells; HGB: hemoglobin; HCT: hematocrit; MCV: mean corpuscular volume; PLT: platelets; ALT: alanine-aminotransferase; AST: aspartate-aminotransferase.

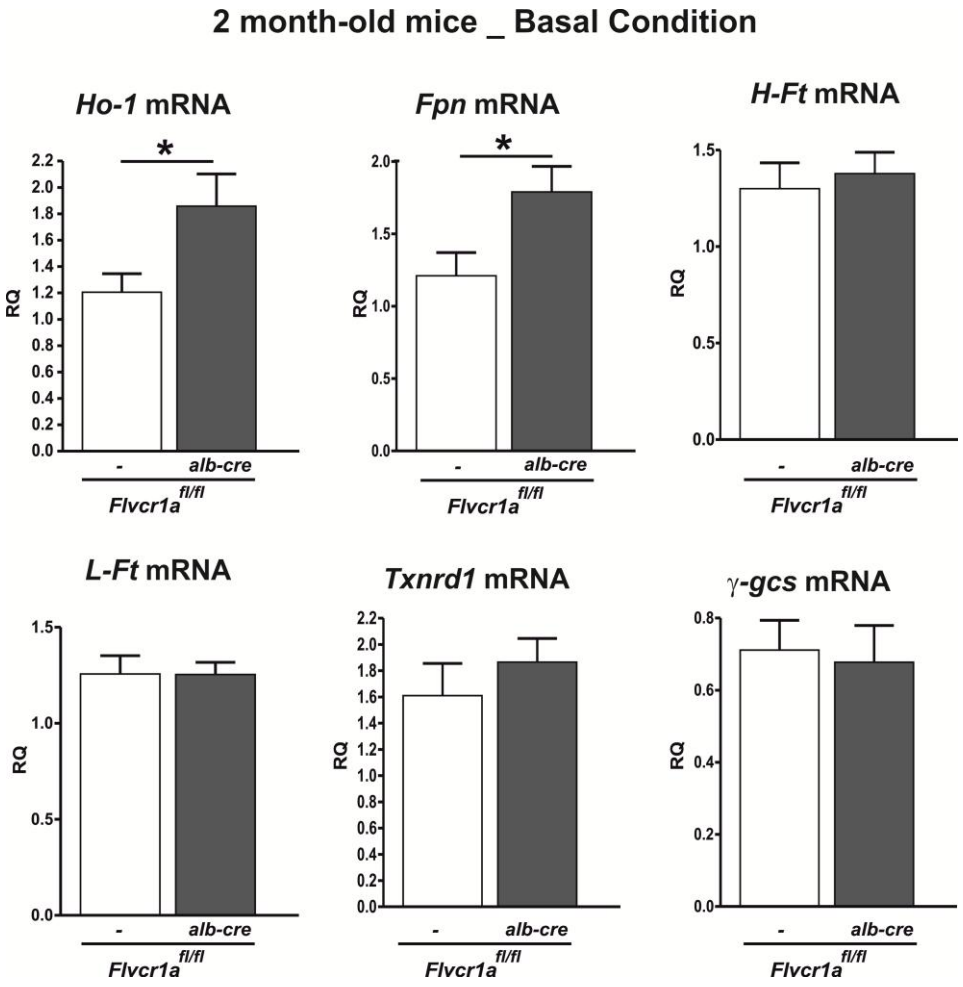

Figure S2. *Flvcr1a* deletion in the liver alters hepatic heme/iron homeostasis in 2 month-old mice. qRT-PCR analysis of *Ho-1*, *Fpn*, *H-Ferritin*, *L-Ferritin*, *Txnrd1 and γ-gcs* mRNA level in the liver of 2 month-old *Flvcr1a*$^{fl/fl}$ and *Flvcr1a*$^{fl/fl}$*;alb-cr*e mice. n=8. Unpaired T-test analysis with Welch's correction was performed on data reported in this figure.

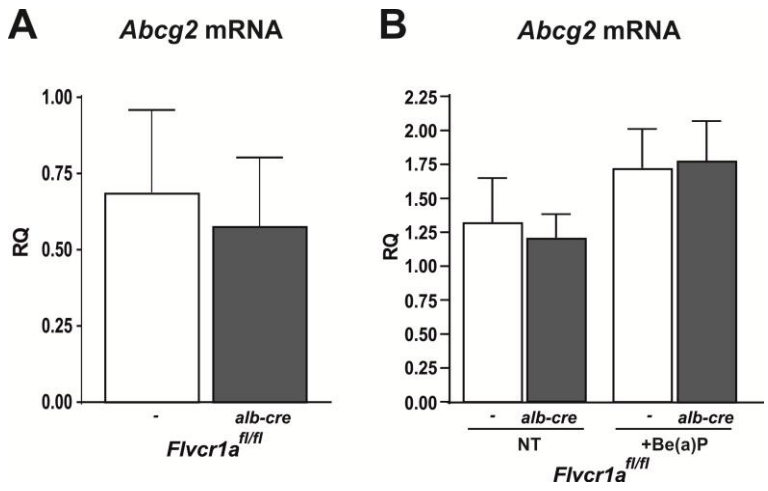

Figure S3. The heme exporter ABCG2 does not compensate for the lack of FLVCR1a function. qRT-PCR analysis of *Abcg2* mRNA level in the liver of 6 month-old *Flvcr1a*$^{fl/fl}$ and *Flvcr1a*$^{fl/fl}$*;alb-cr*e mice (A) and of 2 month-old mice untreated or treated with Be(a)P (B). n=6. Unpaired T-test analysis with Welch's correction was performed on data reported in panel A. Two-way ANOVA with Bonferroni post-test analysis was performed on data reported in panel B.

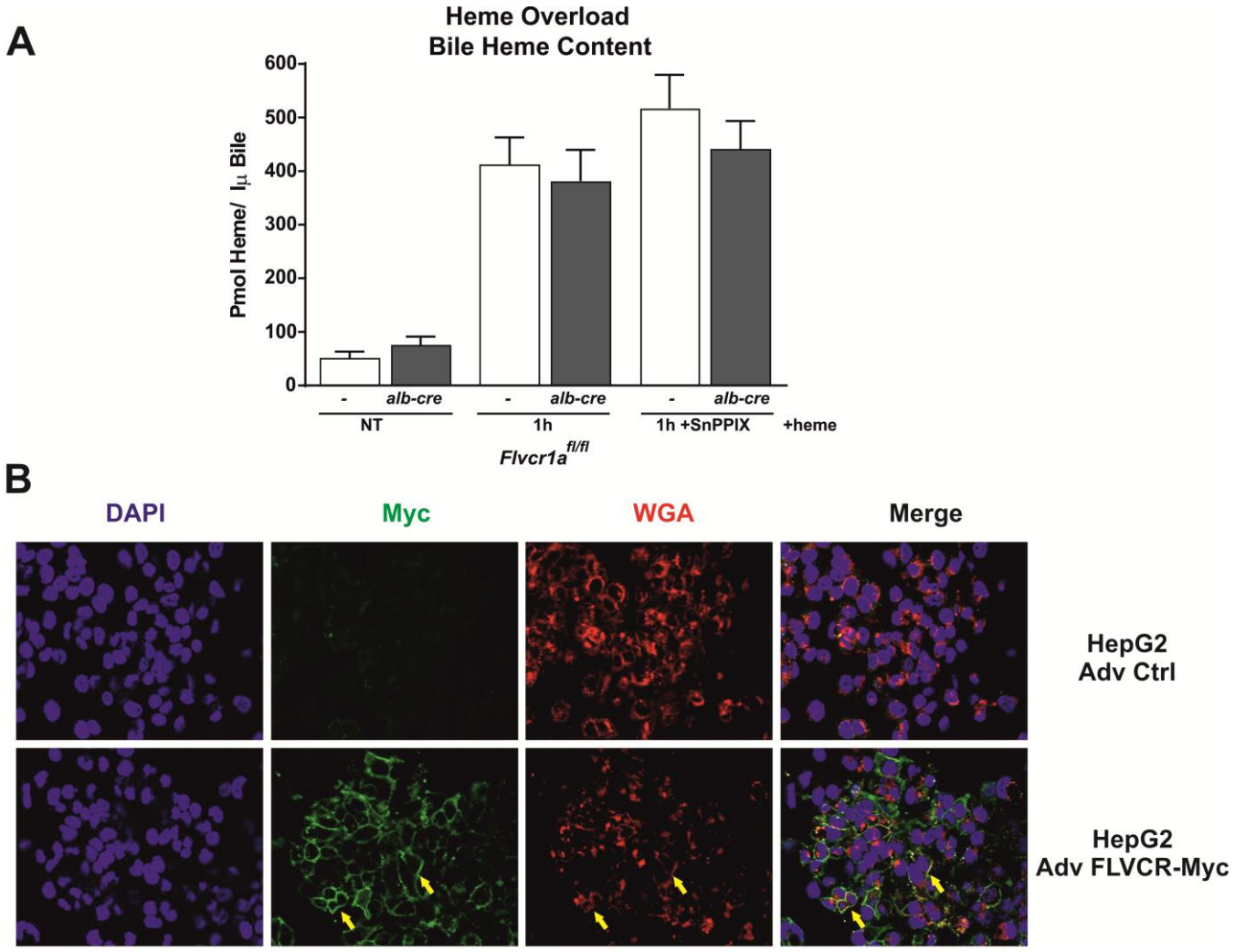

Figure S4. FLVCR1a likely localizes at the sinusoidal membrane of hepatocytes. (A) Quantification of heme content in the bile of *Flvcr1a*$^{fl/fl}$ and *Flvcr1a*$^{fl/fl}$*;alb-cr*e mice upon acute heme overload. After treatment bile was collected from the gallbladder and heme was quantified according to the method described in supplemental method section. After acute heme overload no difference in bile heme content was observed between *Flvcr1a*$^{fl/fl}$ and *Flvcr1a*$^{fl/fl}$*;alb-cr*e mice. The inhibition of HO activity with SnPPIX upon acute heme overload caused an increase in bile heme levels in both *Flvcr1a*$^{fl/fl}$ and *Flvcr1a*$^{fl/fl}$*;alb-cr*e mice, without any remarkable difference. n=6. Two-way ANOVA with Bonferroni post-test analysis was performed on data reported here. (B) Representative images of an immunofluorescence on human hepatocarcinoma HepG2 cells overexpressing Flvcr1a-Myc protein. Cells were stained with DAPI for nuclei identification, an anti-Myc antibody for Flvcr1a-Myc staining and WGA, a dye specific for membranes.
Together these results suggest that FLVCR1a localizes at the hepatic sinusoidal membrane. This needs to be confirmed in vivo when a specific antibody for mouse FLVCR1a will be available.

FLVCR1a deficiency does not affect the response to PHZ-induced hemolysis

We did not observe any difference in heme and iron content (Figure S5A,B) as well as in Ferritin expression and lipid peroxidation (Figure S5C,D) in the liver of *Flvcr1a*$^{fl/fl}$*;alb-cre* mice compared to *Flvcr1a*$^{fl/fl}$ counterpart after 1 month-PHZ treatment, indicating that liver specific *Flvcr1a*-null mice responded to chronic hemolysis similarly to wild-type mice. This was further supported by the observation that *Ho-1* as well as *Fpn* were induced to the same extent in both *Flvcr1a*$^{fl/fl}$*;alb-cre* and *Flvcr1a*$^{fl/fl}$ mice after PHZ treatment and that *Flvcr1a* was strongly downregulated in the liver of PHZ-treated wild-type mice, leading these mice almost to a *Flvcr1a* knock-out condition (Figure S5E). These results suggest that FLVCR1a function is not essential to detoxify heme excess coming from the bloodstream during hemolytic events. This conclusion is further supported by the observation that *Flvcr1a* expression was strongly suppressed in the liver of two mouse models of hemolytic pathologies, Sickle Cell anemia mice and β-thalassemia mice (Figure S5F).

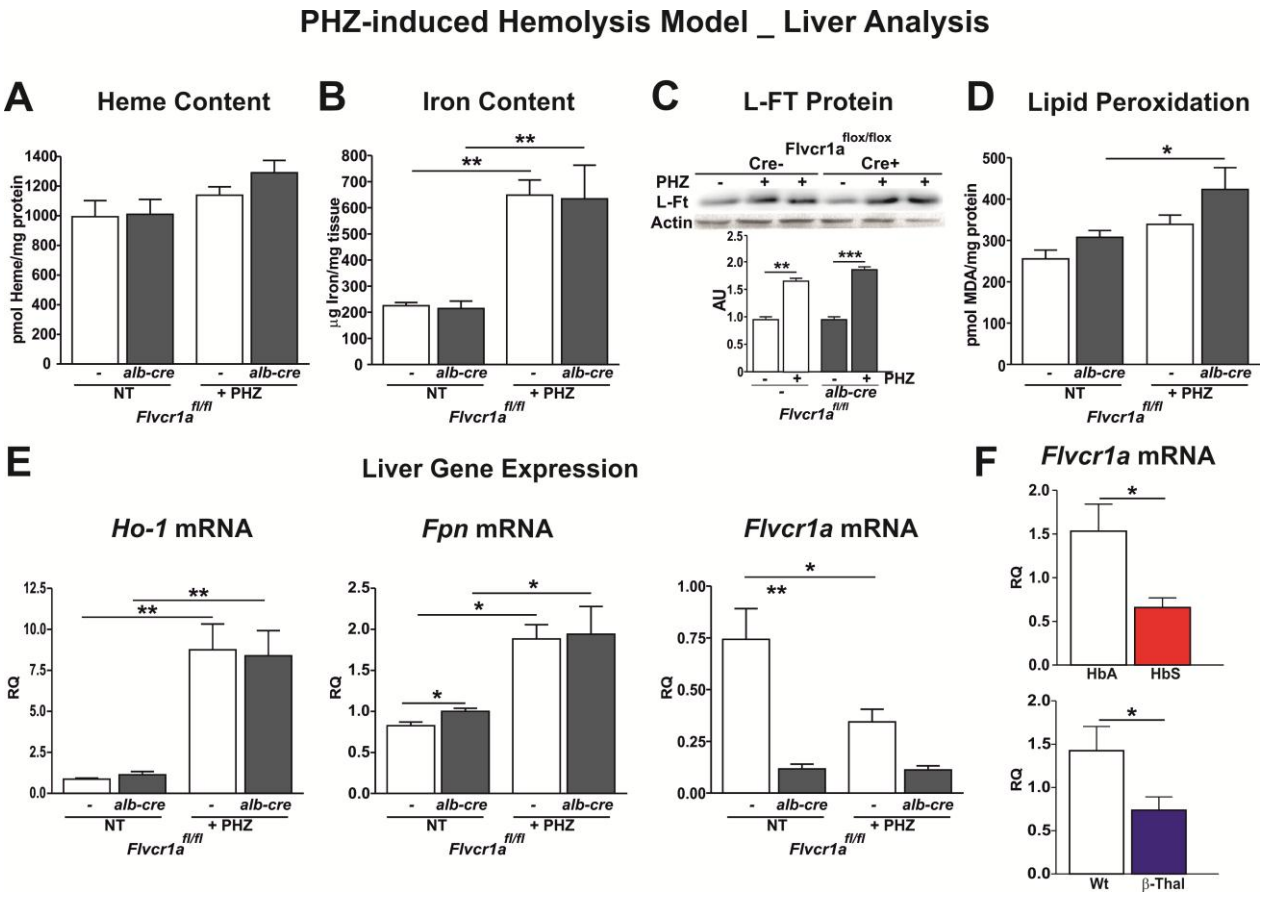

Figure S5. FLVCR1a deficiency does not affect the response to PHZ-induced hemolysis. Heme (A) and iron (B) content, L-Ft expression (C) and MDA content (D) in the liver of *Flvcr1a*$^{fl/fl}$ and *Flvcr1a*$^{fl/fl}$*;alb-cr*e mice after 1-month treatment with PHZ. n=4. (E) qRT-PCR analysis of *Ho-1*, *Fpn* and *Flvcr1a* mRNA level in the liver of *Flvcr1a*$^{fl/fl}$ and *Flvcr1a*$^{fl/fl}$*;alb-cr*e mice after 1-month treatment with PHZ. n=4. (F) qRT-PCR analysis of *Flvcr1a* mRNA level in the liver of sickle and thalassemic mice compared to their respective controls. (NT:n=8; +PHZ n=6). Two-way ANOVA with Bonferroni post-test analysis was performed on data reported in this figure.

In vitro experiments on ALA-treated Primary Hepatocytes confirm in vivo results on ALA-treated *Flvcr1a*$^{fl/fl}$*;alb-cr*e mice

In vitro experiments on primary hepatocytes confirmed the importance of FLVCR1a upon enhanced heme biosynthesis. Hepatocytes prepared from *Flvcr1a*$^{fl/fl}$*;alb-cr*e liver and treated with ALA, accumulated an higher amount of heme compared to cells isolated from *Flvcr1a*$^{fl/fl}$ liver and this was associated to an enhanced production of reactive oxygen species (ROS), indicating an increased oxidative stress (Figure 3D,E). This effect was almost completely abrogated by co-treatment with ALA and the inhibitor of heme biosynthesis, succynilacetone (Figure 3D,E). Consistently with in vivo findings, ALA treatment induced an higher upregulation of *Ho-1*, *H-* and *L-Ferritin* in hepatocytes isolated from *Flvcr1a*$^{fl/fl}$*;alb-cr*e mice compared to those from *Flvcr1a*$^{fl/fl}$ mice (Figure 3F). These data collectively indicate that FLVCR1a-mediated heme export function is strictly associated with heme synthesis.

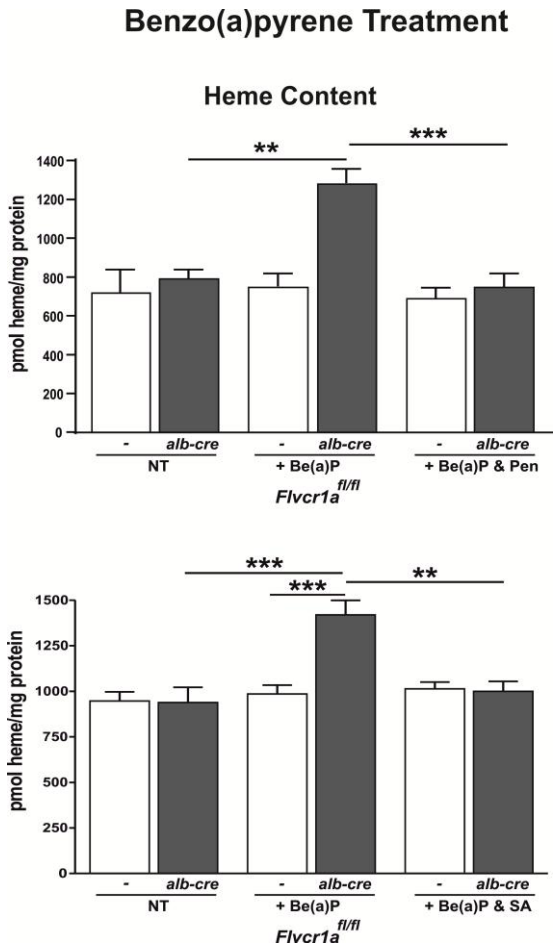

Figure S6. Heme synthesis inhibition blocks heme accumulation in the liver of mice upon Be(a)P treatment. Heme content in the liver of *Flvcr1a*$^{fl/fl}$ and *Flvcr1a*$^{fl/fl}$*;alb-cr*e mice after Be(a)P treatment. Animals were treated with Be(a)P alone or plus the heme synthesis inhibitors DL-Penicillamine or Succynilacetone. Heme accumulation in *Flvcr1a*$^{fl/fl}$*;alb-cr*e mice is blocked by co-treatment with both heme synthesis inhibitors, acting at different levels along the heme biosynthetic pathway. n=6. Two-way ANOVA with Bonferroni post-test analysis was performed on data reported in this figure.

FLVCR1a-mediated heme export function is associated with CYP2E1 induction

Mice were injected with Imidazole, an inducer of CYP2E1, for 4 days. Imidazole treatment caused an increase in heme content in the liver of *Flvcr1a*$^{fl/fl}$*;alb-cr*e mice, that was significantly attenuated in *Flvcr1a*$^{fl/fl}$ counterpart (Figure S7A), further supporting the idea that FLVCR1a is important to export heme upon cytochrome P450 induction. This effect was almost completely abrogated by treatment with Imidazole plus the inhibitor of heme biosynthesis, succynilacetone (Figure S7A). As a consequence of heme accumulation, the liver of *Flvcr1a*$^{fl/fl}$*;alb-cr*e mice accumulated an higher amount of lipid peroxides upon Imidazole treatment compared to *Flvcr1a*$^{fl/fl}$ mice (FigureS7B). The analysis of gene expression by q-RT PCR demonstrated that *Flvcr1a* was induced in the liver of *Flvcr1a*$^{fl/fl}$ mice after Imidazole treatment, as we observed upon Dexamethasone or Be(a)P treatment (Figure S7C). On the other hand, the heme- and iron-related genes were induced to an higher extent in the liver of Imidazole-treated *Flvcr1a*$^{fl/fl}$*;alb-cr*e mice compared to *Flvcr1a*$^{fl/fl}$ counterpart, suggesting that the higher induction of these genes compensated for the lack of *Flvcr1a* induction in the liver of *Flvcr1a*$^{fl/fl}$*;alb-cr*e mice (Figure S7C,D). Moreover, genes involved in heme biosynthesis such as *Alas-1*, *Flvcr1b* and *TfR1* were significantly down-regulated in *Flvcr1a*$^{fl/fl}$*;alb-cr*e mice compared to *Flvcr1a*$^{fl/fl}$ animals, suggesting that the attenuation of the heme biosynthestic pathway may be an attempt to compensate for the excess of heme accumulated in the liver of *Flvcr1a*-deleted mice (Figure S7E). Upon Imidazole treatment, HO-1 activity was significantly higher, whereas ALAS1 expression/activity was markedly reduced in the liver of *Flvcr1a*$^{fl/fl}$*;alb-cr*e mice compared to *Flvcr1a*$^{fl/fl}$ counterparts (Figure S10A,B). As found in Dexamethasone- or Be(a)P-treated mice, cytosolic heme and microsomal heme were significantly higher and lower respectively, in *Flvcr1a*$^{fl/fl}$*;alb-cre* mice than in *Flvcr1a*$^{fl/fl}$ animals (Figure S10C). This correlated with a reduced CYP2E1 activity in the liver of *Flvcr1a*$^{fl/fl}$*;alb-cre* mice (Figure S10E). As expected, *Cyp2e1*

mRNA level in Imidazole-treated animals was not increased since the expression of this gene is mainly regulated at post-transcriptional level (Figure S10D).

These results strengthen those obtained with Dexamethasone or Be(a)P treatment, suggesting that the lack of *Flvcr1a* affects the activity of a wide range of cytochromes.

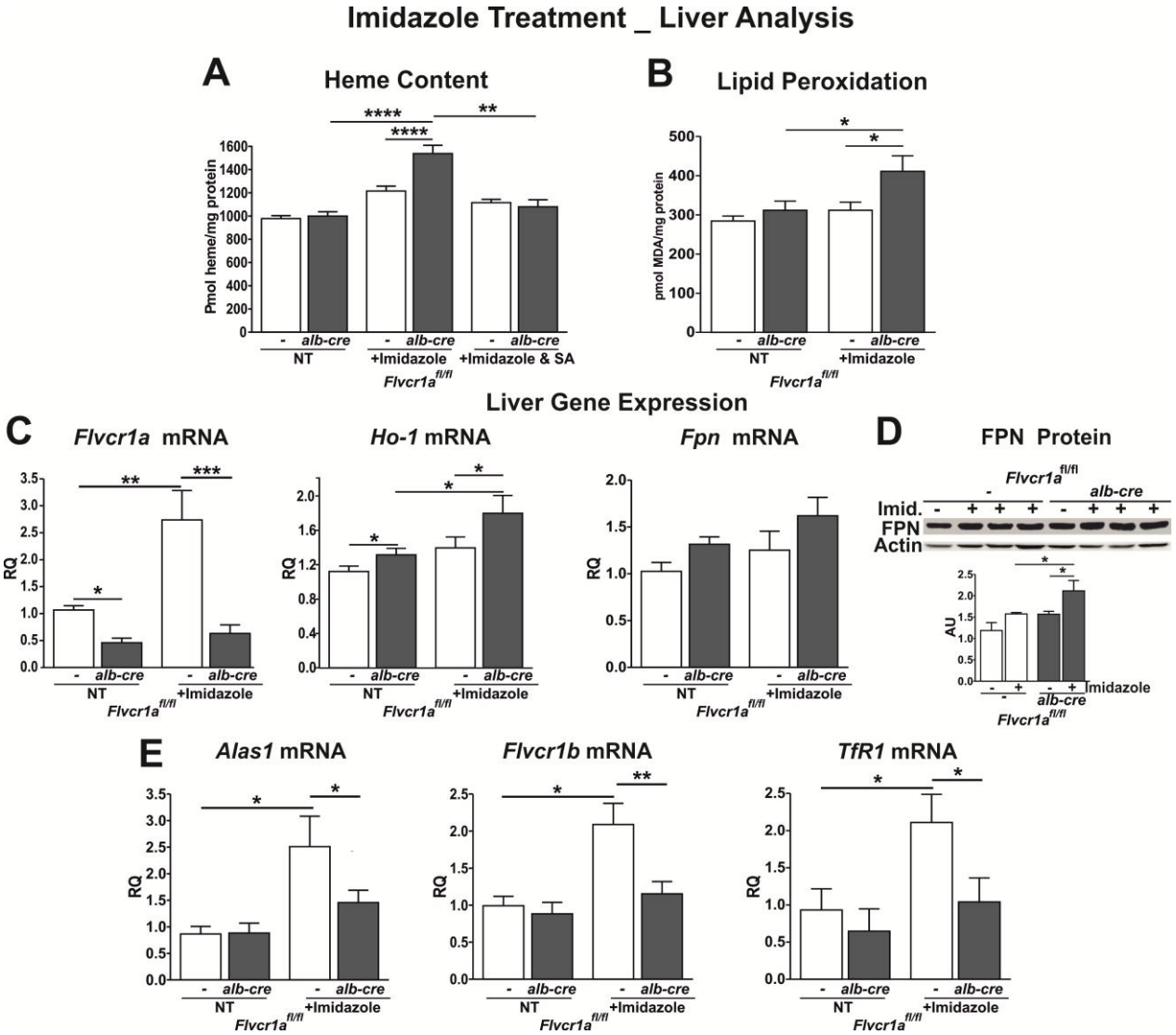

Figure S7. FLVCR1a deficiency affects liver homeostasis following Imidazole-induced cytochrome synthesis. Data on Imidazole-treated *Flvcr1a*$^{fl/fl}$ and *Flvcr1a*$^{fl/fl}$*;alb-cr*e mice are shown. Heme (A) and MDA (B) content in the liver, A:n=10; B:n=6. (C, E) qRT-PCR analysis of *Flvcr1a*, *Ho-1*, *Fpn* and of *Alas1*, *Flvcr1b*, *TfR1* mRNA level in the liver. (NT:n=7; +Imidazole n=15). (D) Representative Western blot showing FPN expression in the liver, n=4. Two-way ANOVA with Bonferroni post-test analysis was performed on data reported in this figure.

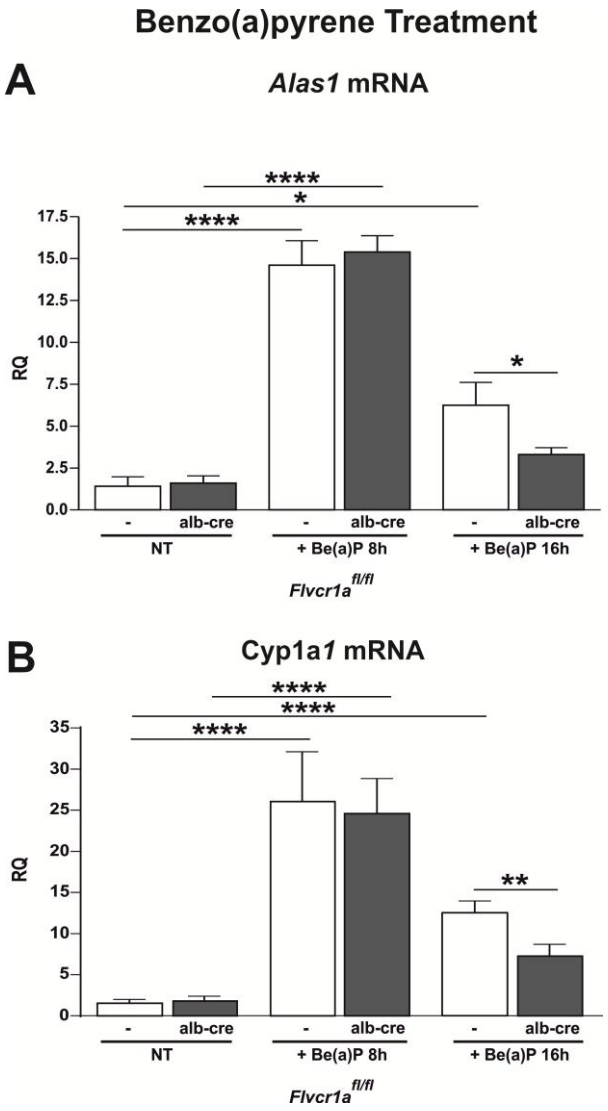

Figure S8. Kinetics of *Alas1* and *Cyp1a1* mRNA induction in the liver of Be(a)P-treated mice. qRT-PCR analysis of *Alas1* (A) and *Cyp1a1* (B) mRNA level in the liver of *Flvcr1a*$^{fl/fl}$ and *Flvcr1a*$^{fl/fl}$*;alb-cr*e mice 8 and 16 hours after Be(a)P treatment. n=6. Two-way ANOVA with Bonferroni post-test analysis was performed on data reported in this figure.

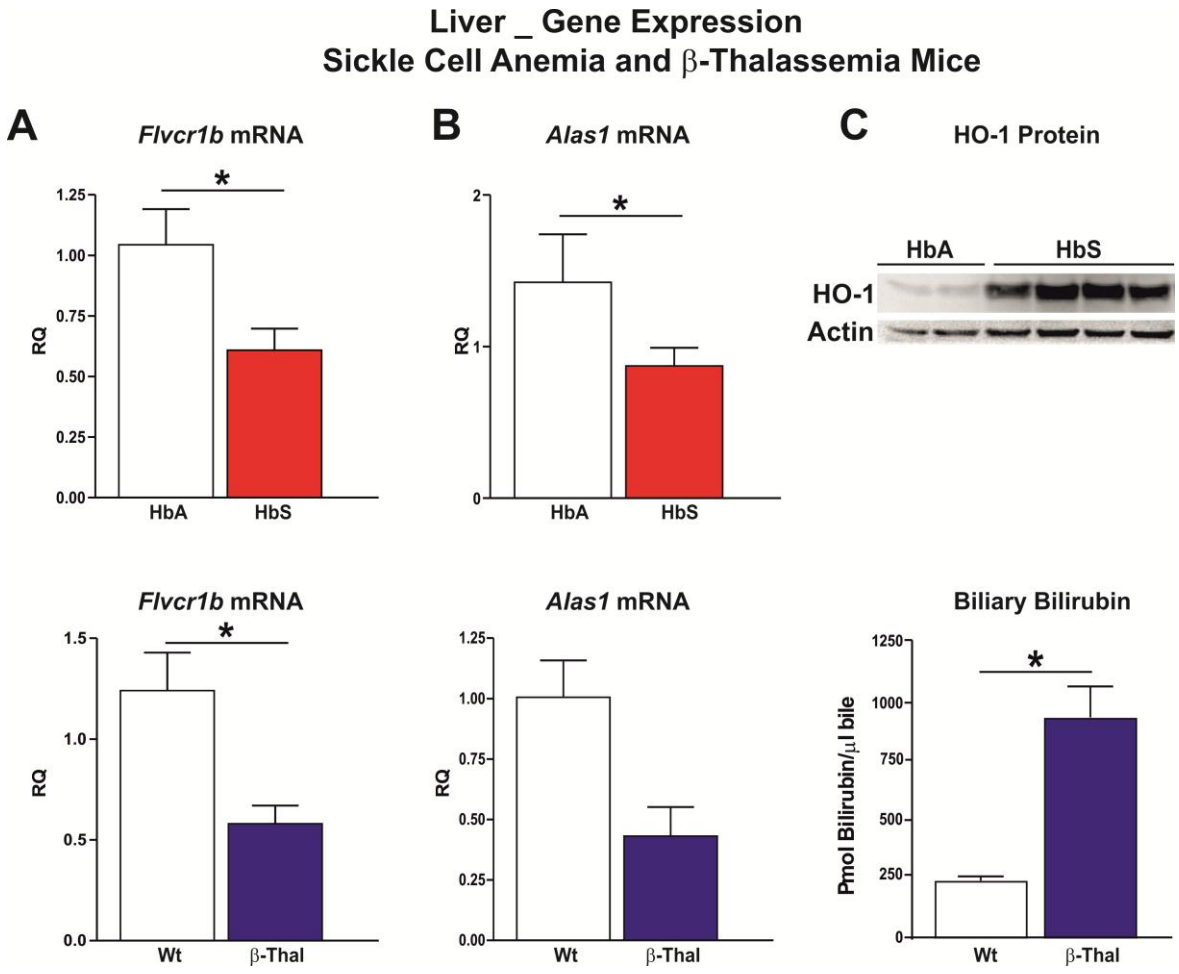

Figure S9. *Flvcr1a* downregulation in Sickle Cell Anemia and β-Thalassemic mice correlates with *Flvcr1b* and *Alas1* downregulation. qRT-PCR analysis of *Flvcr1b* (A) and *Alas1* (B) mRNA level in the liver of Sickle Cell Anemia (upper panel) and β-Thalassemia (bottom panel) mice vs their respective controls. (C) Representative western blot analysis of HO1 expression in the liver of Sickle Cell Anemia mice (upper panel) and bilirubin content in the bile of Thalassemia mice (bottom panel). n=6. Unpaired T-test analysis with Welch's correction was performed on data reported in this figure.

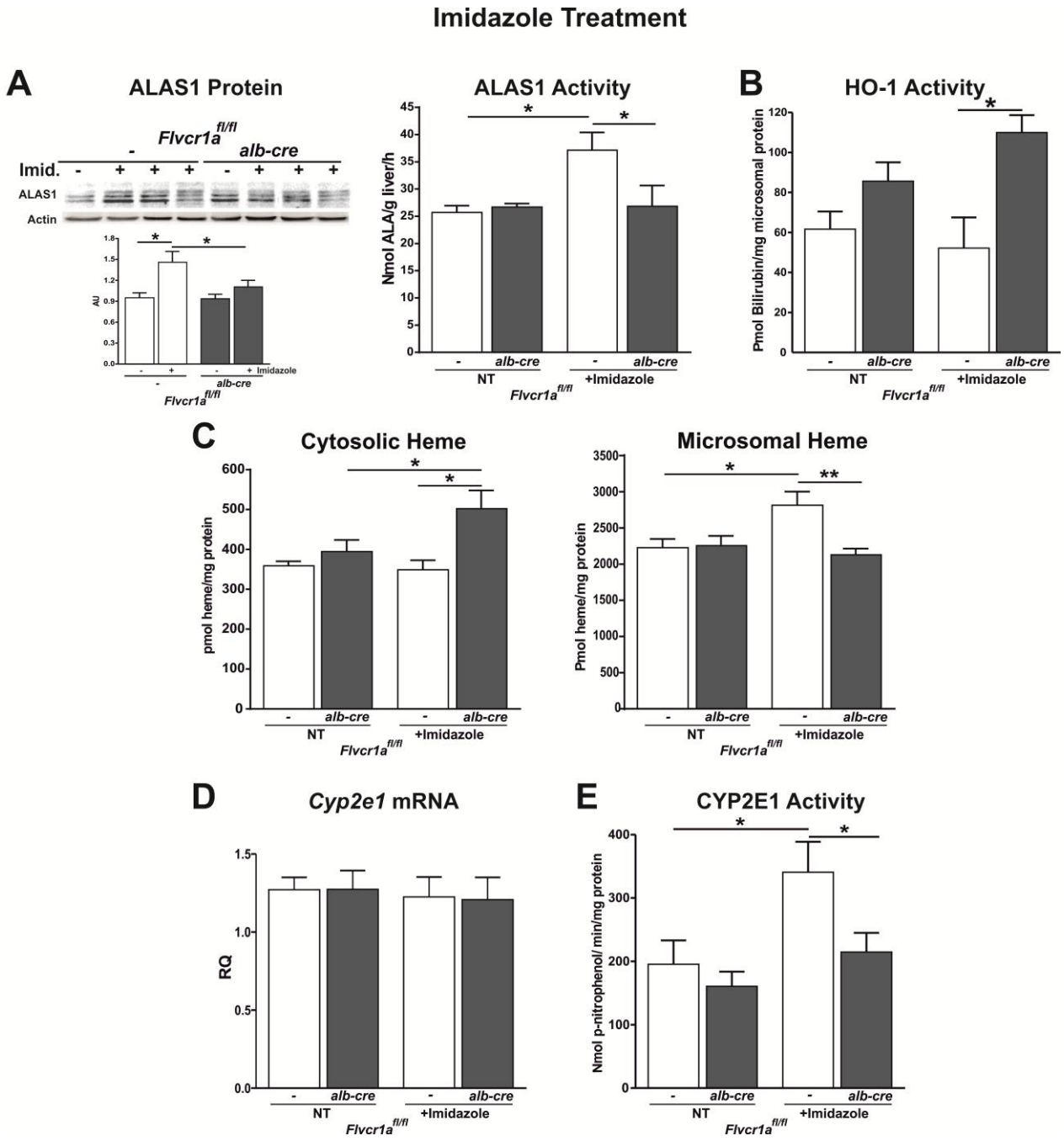

Figure S10. The increase of cytosolic heme pool size due to *Flvcr1a* deficiency inhibits ALAS1 and induces HO activity, thus impairing CYP2E1 activity. Data on Imidazole-treated *Flvcr1a*$^{fl/fl}$ and *Flvcr1a*$^{fl/fl}$*;alb-cr*e mice are shown. (A) Representative Western blot showing ALAS1 expression and ALAS Activity in the liver of, n=8. (B) HO Activity in the liver, n=8. (C) Cytosolic and microsomal heme content in the liver, n=5. (D) qRT-PCR analysis of Cyp2e1 mRNA level (E) CYP2E1 activity in the liver, n=7. Two-way ANOVA with Bonferroni post-test analysis was performed on data reported in this figure.

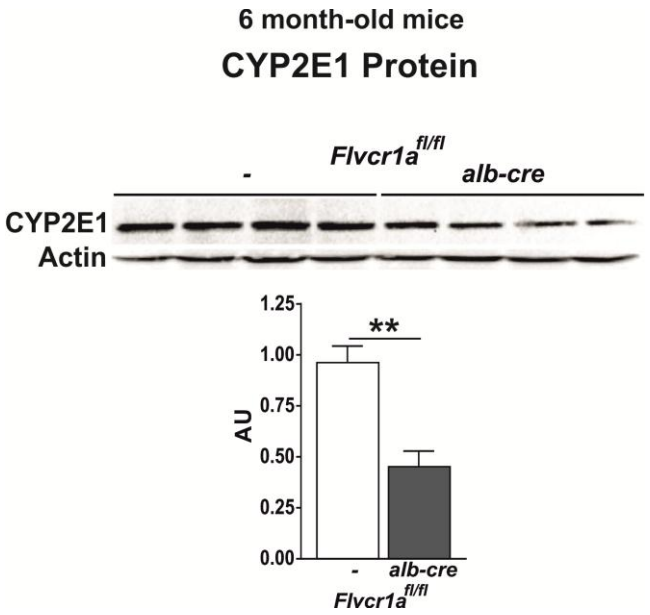

Figure S11. *Flvcr1a* deficiency affects CYP2E1 expression in the liver. Representative Western blot showing CYP2E1expression in the liver of 6 month-old *Flvcr1a*$^{fl/fl}$ and *Flvcr1a*$^{fl/fl}$*;alb-cre* mice, n=4. Unpaired T-test analysis with Welch's correction was performed on data reported. CYP2E1 expression is reduced in *Flvcr1a*$^{fl/fl}$*;alb-cre* mice as well as CYP1A1 and CYP3A expression, as shown in Figure 7D.

Supplemental legend for Figure7F

Figure 7F. Cartoon showing FLVCR1a mood of action in the liver. Upon steady state condition (*left*), heme is synthesized by ALAS1 and enters the free heme pool, in which it is dinamically exchanged between the regulatory and the active pool contained in hemoproteins. The heme pool is maintained by a balance between heme synthesis, degradation and export thanks to the coordinated activity of ALAS1, HO1 and FLVCR1a. This ensures a proper size of the heme pool that reflects the functionality of the major group of hepatic hemoproteins, cytochromes P450. The deletion of the heme exporter FLVCR1a (*right*) alters intracellular heme homeostasis, thus impairing this balance. The enhacement in heme pool size due to the lack of heme export causes, on the one hand, the compensatory upregulation of HO1 and, on the other, the compensatory inhibition of ALAS1. This leads to an increase in heme degradation and a decrease in *de novo* heme synthesis, thus resulting in impaired CYP450 expression and activity.

Supplemental references

1. Vinchi, F., De Franceschi, L., Ghigo, A., Townes, T., Cimino, J., Silengo, L., Hirsch, E., Altruda, F., and Tolosano, E. 2013. Hemopexin therapy improves cardiovascular function by preventing heme-induced endothelial toxicity in mouse models of hemolytic diseases. *Circulation* 127:1317-1329.
2. Chiabrando, D., Marro, S., Mercurio, S., Giorgi, C., Petrillo, S., Vinchi, F., Fiorito, V., Fagoonee, S., Camporeale, A., Turco, E., et al. 2012. The mitochondrial heme exporter FLVCR1b mediates erythroid differentiation. *J Clin Invest* 122:4569-4579.
3. Borova, J., Fuchs, O., Hradilek, A., and Neuwirt, J. 1984. Effect of hemin and heme synthesis inhibitors on cellular protein synthesis. *Biomed Biochim Acta* 43:11-21.
4. Goncalves, L.A., Vigario, A.M., and Penha-Goncalves, C. 2007. Improved isolation of murine hepatocytes for in vitro malaria liver stage studies. *Malar J* 6:169.
5. Sassa, S. 1976. Sequential induction of heme pathway enzymes during erythroid differentiation of mouse Friend leukemia virus-infected cells. *J Exp Med* 143:305-315.
6. Pieroni, L., Khalil, L., Charlotte, F., Poynard, T., Piton, A., Hainque, B., and Imbert-Bismut, F. 2001. Comparison of bathophenanthroline sulfonate and ferene as chromogens in colorimetric measurement of low hepatic iron concentration. *Clin Chem* 47:2059-2061.
7. Marver, H.S., Tschudy, D.P., Perlroth, M.G., and Collins, A. 1966. Delta-aminolevulinic acid synthetase. I. Studies in liver homogenates. *J Biol Chem* 241:2803-2809.
8. Burke, M.D., Thompson, S., Elcombe, C.R., Halpert, J., Haaparanta, T., and Mayer, R.T. 1985. Ethoxy-, pentoxy- and benzyloxyphenoxazones and homologues: a series of substrates to distinguish between different induced cytochromes P-450. *Biochem Pharmacol* 34:3337-3345.
9. Koop, D.R. 1986. Hydroxylation of p-nitrophenol by rabbit ethanol-inducible cytochrome P-450 isozyme 3a. *Mol Pharmacol* 29:399-404.